OncoTargets and Therapy

Dovepress
open access to scientific and medical research

Open Access Full Text Article

ORIGINAL RESEARCH

SKF95365 induces apoptosis and cell-cycle arrest by disturbing oncogenic Ca^{2+} signaling in nasopharyngeal carcinoma cells

This article was published in the following Dove Press journal:
OncoTargets and Therapy
27 October 2015
Number of times this article has been viewed

Jinyan Zhang[1]
Jiazhang Wei[2]
Qian He[3]
Yan Lin[1]
Rong Liang[1]
Jiaxiang Ye[1]
Zhe Zhang[4]
Yongqiang Li[1]

[1]Department of Medical Oncology, Affiliated Cancer Hospital of Guangxi Medical University, [2]Department of Otolaryngology-Head and Neck Oncology, The People's Hospital of Guangxi Zhuang Autonomous Region, Nanning, People's Republic of China; [3]Graduate School of Information Science and Technology, Hokkaido University, Sapporo, Japan; [4]Department of Otolaryngology-Head & Neck Surgery, First Affiliated Hospital of Guangxi Medical University, Nanning, People's Republic of China

Background: Aberrant modulation of store-operated calcium ions (Ca^{2+}) entry promotes the progression of human malignancies. Previously, we reported that the blockage of store-operated Ca^{2+} entry inhibited epidermal growth factor (EGF)-stimulated migration and distant metastasis in nasopharyngeal carcinoma (NPC) cells. However, the effects of pharmacological blocker on other Ca^{2+} signaling-regulated malignant characteristics in NPC cells remained poorly understood.

Methods: We examined the effects of SKF96365, an inhibitor of store-operated Ca^{2+} channel, on EGF-launched Ca^{2+} signaling in two NPC cell lines. We determined the effects of SKF96365 on cell proliferation, colony formation, apoptosis, and cell-cycle status in vitro. We further elucidated the antitumor activity of SKF96365 in xenograft-bearing mice.

Results: It was found that SKF96365 disturbed the thapsigargin (TG)-stimulated Ca^{2+} release from endoplasmic reticulum and the subsequent Ca^{2+} influx. SKF96365 alone stimulated Ca^{2+} responses merely due to endoplasmic reticulum-released Ca^{2+}. SKF96365 promoted cell mortality, inhibited colony formation, and induced apoptosis and cell-cycle arrest, while blunting the EGF-evoked Ca^{2+} signaling. Furthermore, we confirmed that SKF96365 reduced NPC xenograft growth while activating caspase-7-related apoptotic pathway.

Conclusion: SKF96365 exerts multiple antitumor activities through the distraction on the oncogenic Ca^{2+} signaling transduction in NPC cells.

Keywords: store-operated Ca^{2+} entry, EGF signaling, caspase-7, caspase-9

Introduction

Calcium ions (Ca^{2+}) participate in the regulations of nearly every aspect of cellular life as a unique intracellular second messenger.[1] The elevation of cytosolic Ca^{2+} level ($[Ca^{2+}]_{cyto}$) evoked by extracellular stimuli mediates the signal transductions from exterior into intracellular space and thus drives the downstream pathway, thereby enabling cells to sense the changes of external environment and adjust their functional status appropriately.[1] To ensure that the increase of intracellular Ca^{2+} concentration can be accomplished accurately in response to the extracellular signals, $[Ca^{2+}]_{cyto}$ is carefully controlled and regulated in cytoplasm. Store-operated Ca^{2+} entry (SOCE) is a pattern of cellular Ca^{2+} responses in nonexcitable cells, which is initialized by the binding of extracellular ligand to membrane receptor.[2,3] The activation of receptor triggers the release of Ca^{2+} from intracellular Ca^{2+} store (endoplasmic reticulum [ER]), which is followed by the ER-depletion-stimulated Ca^{2+} influx via the membrane Ca^{2+} channels, thereby consequently achieving the rapid increase in $[Ca^{2+}]_{cyto}$ as required for the downstream signal transductions.[2,3]

Abnormal modulation of SOCE has been demonstrated to be responsible for various human diseases.[4] The crucial role of SOCE in the progressions of human malignancies

Correspondence: Yongqiang Li
Department of Medical Oncology, Affiliated Cancer Hospital of Guangxi Medical University, 71 Hedi Road, Nanning 530021, People's Republic of China
Tel +86 771 533 2578
Fax +86 771 533 2393
Email gxct.ly@gmail.com

submit your manuscript | www.dovepress.com
Dovepress
http://dx.doi.org/10.2147/OTT.S92005

has also been established.[5–8] Nasopharyngeal carcinoma (NPC) is a unique head and neck malignant disease with an extremely unbalanced geographical distribution.[9,10] Epstein–Barr virus infection, regional environmental factors, genetic, and epigenetic modifications synergistically contribute to NPC pathogenesis.[9,10] Previously, we reported that the blockage of SOCE inhibited epidermal growth factor (EGF)-stimulated migration in NPC cells.[11] However, Ca^{2+} signaling regulates not only cell motility but also other malignant properties in cancer cells.[12,13] The present study was designed to examine the effects of SKF96365, a pharmacological blocker of Ca^{2+} release-activated Ca^{2+} entry, on cell mortality, colony formation, apoptosis, and cell-cycle status in NPC cells. We further estimated the in vivo antitumor effect of SKF95365 on tumorigenesis in xenograft-bearing mice. This study aimed to explore the potential antitumor activities that were attributable to the distinct impact of SKF96365 on Ca^{2+} signaling in NPC cells.

Materials and methods

Cell culture

The use of human NPC cell lines was approved by the ethics committee of Guangxi Medical University. The informed consent form was obtained from the donors. Human NPC cell lines CNE2 and HONE1 were cultured in Dulbecco's Modified Eagle's Medium/Nutrient Mixture F-12 (DMEM/F-12, Thermo Fisher Scientific, Waltham, MA, USA) supplemented with 5% fetal bovine serum (FBS), penicillin at 100 U/mL, and streptomycin at 100 μg/mL (Thermo Fisher Scientific). The cells were routinely maintained in an incubator at 37°C under 5% CO_2.

Drug and solution

1-[2-(4-Methoxyphenyl)-2-[3-(4-methoxyphenyl)propoxy] ethyl]imidazole and 1-[β-(3-(4-methoxyphenyl)propoxy)-4-methoxyphenethyl]-1H-imidazole hydrochloride (SKF95365) were purchased from Sigma-Aldrich Co. (St Louis, MO, USA). To avoid any bias resulting from the different amount of dimethyl sulfoxide (DMSO) used, SKF96365 was dissolved in DMSO at various concentrations as stock solutions (1 mmol/L, 5 mmol/L, 10 mmol/L, 1,000-fold), which were further added into the medium or phosphate-buffered saline (PBS) (1:1,000 dilution) before the experiments, respectively, with pH 7.4 at 25°C. Thus, the amounts of DMSO added into each group were equalized. Equal amount of DMSO without SKF96365 was applied into the medium as vehicle control (denoted as 0 μmol/L).

Measurement of cytosolic Ca^{2+}

To avoid any undefined stimuli to affect $[Ca^{2+}]_{cyto}$, the cells were incubated in serum-free medium for 24 hours before the measurement of $[Ca^{2+}]_{cyto}$. $[Ca^{2+}]_{cyto}$ was measured in individual NPC cells utilizing a fluorescent Ca^{2+} indicator, the acetoxymethyl ester of fura-2 (fura-2/AM; Dojindo Molecular Technologies, Inc., Kumamoto, Japan), as described in our previous studies.[11,14,15] The absorption shift of fura-2 that occurs upon binding can be determined by scanning the excitation spectrum between 340 nm and 380 nm while monitoring the emission at 510 nm. Fluorescent images were acquired and quantified from the individual fura-2-loaded cells with a fluorescence imaging and analysis system (Aqua Cosmos 2.6; Hamamatsu Photonics, Hamamatsu, Japan). Changes in the fluorescence ratio (F340/F380) represented the changes in $[Ca^{2+}]_{cyto}$.

3-(4,5-Dimethylthiazol-2-yl)-2,5-diphenyltetrazolium bromide assay

Cell mortality was determined using the 3-(4,5-dimethylthiazol-2-yl)-2,5-diphenyltetrazolium bromide (MTT) assay kit (Thermo Fisher Scientific), as our earlier description.[16] The NPC cells were seeded onto a 96-well plates at a density of 5×10^3 cells per well. The adherent growing cells were supplemented with DMEM/F-12 with 5% FBS, EGF at 50 ng/mL, and incubated with SKF96365 at various concentrations for 48 hours. The cell number was determined as the absorbance at 570 nm with a spectrophotometer according to the manufacturer's protocol.

Colony-forming assay

A total of 1×10^3 cells were suspended and seeded onto each 60-mm cell culture dish. The cells were incubated in DMEM/F-12 with 5% FBS. The mediums containing EGF at 50 ng/mL and SKF96365 at increasing concentrations were applied at 24 hours postseeding and replaced daily. After 14 days of incubation, the colonies were fixed with 4% paraformaldehyde and stained with 0.2% crystal violet. The colonies were photographed under an inverted microscope, and the number of colonies was counted using Quantity One software (Bio-Rad Laboratories, Inc., Hercules, CA, USA).

Cell apoptosis assay

The status of cell apoptosis was examined using an Annexin V-FITC/propidium iodide (PI) cell apoptosis assay kit (Keygen Inc., Nanjing, People's Republic of China), as described in our previous study.[16] Briefly, the cells cultured on six-well plates were treated with SKF96365 at increasing concentrations for 48 hours. The cells were harvested and washed with PBS solution and resuspended in the binding buffer, incubated with AnnexinV-FITC and PI in the dark for 15 minutes. The fluorescence was detected by means of flow

cytometry (excitation wavelength [Ex] =488 nm; emission wavelength [Em] =530 nm). The Annexin V-FITC-positive and PI-negative cells were defined as early apoptotic cells, and Annexin V-FITC-positive and PI-positive cells were considered as late apoptotic cells. The status of cell apoptosis was quantitatively estimated by comparing the total percentage of the apoptotic cells present.

Caspase activity assays

The activities of caspase-7 and caspase-9 were estimated by using homogeneous caspase assay and Caspase-Glo® 9 Assay Kits (Promega Corporation, Fitchburg, WI, USA), respectively. In brief, cell lysates harvested from vehicle control or SKF96365-treated cells were used for the caspase activity assays. Assays were carried out on 96-well plates, and the activities were determined quantitatively as the fluorescence from each well according to the manufacturer's instructions.

Western blotting

Pro- and cleaved caspase-7 expressions were examined using Western blot (anti-procaspase-7 and anticleaved caspase-7 antibodies, 1:200 dilution; Abcam Corp., Cambridge, UK), according to the standard protocol. β-Actin expression served as internal controls (anti-β-actin antibody, 1:500 dilution; Abcam Corp.). For the blotting, each lane was loaded with 50 μg of protein. The blots were visualized using enhanced chemiluminescence detection (Pierce, Rockford, IL, USA).

Cell-cycle analysis

Cell-cycle stage was determined by means of flow cytometry using a cell-cycle assay kit (Keygen Inc.). After PI staining, the cellular DNA content was determined according to the manufacturer's instruction. The cells were distinguished as being at the G0/G1, G2/M, and S phases of the cell cycle based on the fluorescence intensity, and the distribution of cell-cycle stage was analyzed using Cell-FIT software (BD Biosciences, San Jose, CA, USA).

Nude mouse xenograft

A total of 5×10^6 CNE2 cells were trypsinized and resuspended in sterile PBS and subcutaneously inoculated into the right flank of each nude mouse (Japan SLC, Inc., Hamamatsu, Japan). Six mice were assigned into SKF96365-treated or vehicle control group. The palpable xenografts could be observed on day-10 postinoculations, when SKF96365 or PBS was intraperitoneally injected daily at 10 mg/kg in each mouse for 20 days. The tumor dimensions were measured every 7 days using a vernier caliper, and the tumor volumes were calculated according to the formula: $V = (W^2 \times L)/2$, where W is the width and L is the length of a xenograft. At the end of the observation of tumor growth, the mice were anesthetized and perfused with PBS with 4% paraformaldehyde, and then the mice were sacrificed and the xenografts were isolated. The xenografts tissues were subjected to routine paraffin-embedded section and followed by immunohistochemical analysis of cleaved caspase-7. All the in vivo experiments performed in our study conformed to the Guide for the Care and Use of Laboratory Animals published by the US National Institutes of Health (NIH publication, eighth edition, 2010). All experiments were performed in accordance with the regulations of the Animal Research Committee of Guangxi Medical University.

Statistics

The concentration–response data were fitted, and half maximal inhibitory concentration (IC_{50}) and Hill coefficient values were obtained using Sigma-Plot 10.0 (Systat Software Inc., Munich, Germany). Unpaired Student's *t*-test was used for statistical analyses. Statistical analyses were performed using Graph Pad Prism 5 (GraphPad Software, Inc., La Jolla, CA, USA). All data were presented as the mean ± standard deviation. Statistical significance was assumed when *P*-values were <0.05.

Results

SKF96365 exhibits dual inhibitory effects on ER-released Ca^{2+} and the following Ca^{2+} influx

The inhibition of SOCE with 2-Aminoethoxydiphenyl borate (2-APB), one of the blockers for SOCE, was shown in our previous work.[11,14] The inhibition of extracellular Ca^{2+} influx induced by 2-APB was confirmed to be independent of the Ca^{2+} release from ER.[14] In the present study, another widely utilized blocker of SOCE, SKF96365, showed inhibitory effect on not only Ca^{2+} influx, but also the upstream Ca^{2+} depletion in ER. As shown in Figure 1A, thapsigargin (TG) (1 μmol/L), a noncompetitive inhibitor of the Ca^{2+}-ATPase located in ER, was used to empty the Ca^{2+} content in this dominated intracellular Ca^{2+} store. Simultaneously applied SKF96365 at 5 μmol/L significantly decreased ER-released Ca^{2+} without affecting the following Ca^{2+} influx in NPC cell line CNE2 but did not significantly modify the ER-released Ca^{2+} in another NPC cell line HONE1 (Figure 1A). Moreover, SKF96365 at 10 μmol/L obviously reduced both the mobilization of Ca^{2+} from ER and the subsequent Ca^{2+} influx in the two cell lines (Figure 1A). In addition, the cells were incubated in Ca^{2+}-free solution with TG for 10 minutes, and

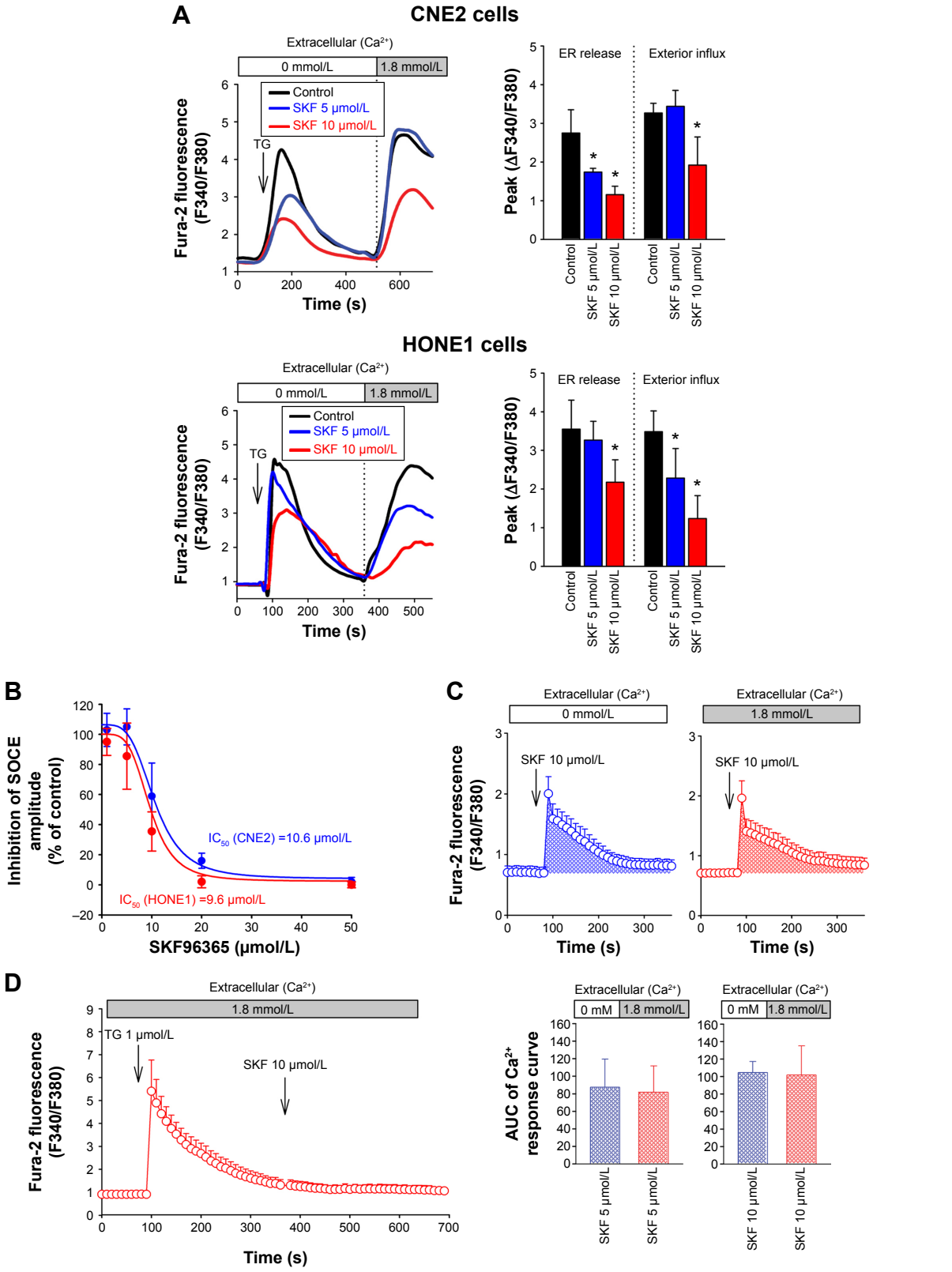

Figure 1 SKF96365 exhibits inhibitory effects on both ER-released Ca^{2+} and the following Ca^{2+} influx.

Notes: (**A**) TG-induced Ca^{2+} release from ER and the Ca^{2+} influx via membrane channels were measured in the absence and presence of extracellular Ca^{2+}, respectively. Cytosolic Ca^{2+} concentration $[Ca^{2+}]_{cyto}$ is shown as the fluorescence ratio (F340/F380) of fura-2. Each trace represents the average data from at least 20 single cells. The Ca^{2+} responses were quantified as the average peak from the baseline in each right panel. (**B**) The dose–response curves of SKF96365 on SOCE amplitude in NPC cells. (**C**) The Ca^{2+} responses elicited by SKF96365 in the absence and presence of extracellular Ca^{2+}. The Ca^{2+} responses were quantified by calculating the AUC in the bottom panel. (**D**) Effect of SKF96365 on cytosolic Ca^{2+} in the ER-Ca^{2+}-depleted cells pretreated with TG. Data are represented as mean ± SD (*$P<0.05$, Student's *t*-test).

Abbreviations: SKF, SKF96365; TG, thapsigargin; AUC, area under the curve; ER, endoplasmic reticulum; SOCE, store-operated Ca^{2+} entry; NPC, nasopharyngeal carcinoma; IC_{50}, half maximal inhibitory concentration; SD, standard deviation; s, seconds.

the increasing concentrations of SKF96365 were applied before the switch to 1.8 mmol/L Ca^{2+} solution. The dose–response curve of SKF96365 on SOCE amplitude is shown in Figure 1B.

On the other hand, whether SKF96365 can directly affect cytosolic Ca^{2+} homeostasis or not in NPC cells remained unknown. To address this issue, CNE2 and HONE1 cells were stimulated by SKF96365 alone. SKF96365 at 10 μmol/L induced a rapid elevating and gradual declining Ca^{2+} responses in the absence of extracellular Ca^{2+} in CNE2 cells (Figure 1C). The similar results were also found in HONE1 cells (data not shown). Furthermore, we confirmed that the Ca^{2+} responses stimulated by SKF96365 in the presence of extracellular Ca^{2+} neither modified the appearance of the Ca^{2+} responses nor increased the quantification of the Ca^{2+} increase (Figure 1C), suggesting that the SKF96365-induced Ca^{2+} increase actually represented the ER-released Ca^{2+} but not the Ca^{2+} influx. To confirm that SKF96365 could only stimulate Ca^{2+} release from ER without affecting Ca^{2+} influx, the NPC cells were pretreated with TG to completely deplete the ER-Ca^{2+} content, and SKF96365 at 10 μmol/L was subsequently applied but failed to affect $[Ca^{2+}]_{cyto}$ in these ER-depleted CNE2 (Figure 1D) and HONE1 cells (data not shown), thus confirmed that SKF96365 could not stimulate Ca^{2+} influx.

SKF96365 increases cell mortality and inhibits colony formation while disturbing EGF-evoked Ca^{2+} signaling

The distinct dual effects on intracellular mobilization of Ca^{2+} and the extracellular Ca^{2+} influx suggested that SKF96365 might have special antitumor potential to affect not only cell migration, as reported previously,[8] but also the other Ca^{2+} signaling-regulated malignant properties in NPC cells.[13] The blockers of SOCE, such as 2-APB, did not show significant inhibition on CNE2 or HONE1 cell mortality as measured by the MTT assay in our earlier study.[11] However, SKF96365 promoted cell mortality in a dose-dependent manner in CNE2 and HONE1 cells (Figure 2A). The maximum inhibition rate was 49.7%±1.4% and 30.1%±3.6% in CNE2 and HONE1 cells, respectively. The IC_{50} for SKF96365 was 2.5 μmol/L and 3.4 μmol/L in CNE2 and HONE1 cells, respectively. SKF96365 also exhibited time-accumulating inhibitory effect on both CNE2 and HONE1 cells (Figure 2B). In addition, SKF96365 inhibited colony formation by 57.1%±7.8% and 63.7%±10.4% at 1 μmol/L in CNE2 and HONE1 cells, respectively, and further inhibited colony formation by 90.3%±4.5% and 90.3%±6.4% at 5 μmol/L in these two cell lines and almost eliminated the clonogenicity at 10 μmol/L (Figure 2C). We also confirmed that long-term treatment (>72 hours) of SKF96365 at 1–10 μmol/L did not induce apparent Ca^{2+} deprivation of the NPC cells by examining the resting $[Ca^{2+}]_{cyto}$ (data not shown).

Epithelial cell mortality and colony formation are regulated by EGF signaling. The results shown in Figure 1A suggested that SKF96365 might influence on both the ER-released Ca^{2+} and extracellular Ca^{2+} influx, thus disturb the Ca^{2+} signaling evoked by the extracellular signal molecule such as EGF. To clarify how SKF96365 modulates EGF-stimulated Ca^{2+} signaling, we examined the effect of preincubation of SKF96365 at 5 μmol/L on EGF-evoked Ca^{2+} responses and found that SKF96365 weakened and desynchronized the EGF-evoked Ca^{2+} signaling in CNE2 and HONE1 cells (Figure 2D). The SKF96365-blunted EGF Ca^{2+} signaling might be responsible for the increased cell mortality and reduced colony formation.

SKF96365 induces apoptosis and cell-cycle arrest at G2/M and S phases

SOCE was demonstrated to regulate cell apoptosis, and the inhibition of SOCE enhanced apoptosis in cancer cells.[7] Here, we determined the effect of SKF95365 on apoptotic status in NPC cells. The apoptosis rate was significantly increased in the SKF95365-treated cells compared with the vehicle control (Figure 3A). Moreover, it was found that the incubation with SKF95365 at 10 μmol/L for 48 hours augmented the activities of both caspase-9 and caspase-7 in CNE2 and HONE1 cells (Figure 3B). In view of the fact that caspase-9 and caspase-7 serve as an initiator and executioner protein during cell apoptosis process, respectively, and it is well-known that caspase-9 is able to cleave inactive procaspase-7, and thereby activating it, we hypothesized that SKF96365 induced apoptosis through the sequential activations of caspase-9 and caspase-7. To further validate this, we performed immune blots to examine the procaspase-7 (inactive) and cleaved caspase-7 (active) expressions in CNE2 and HONE1 cells. We confirmed that SKF95365 increased the cleaved caspase-7 while decreasing the procaspase-7 expression (Figure 3C). Thus, the cleaved caspase-7 activated by caspase-9 contributed to the SKF96365-induced cell apoptosis, and accordingly the SKF96365-triggered apoptotic pathway was preliminarily identified.

Furthermore, the treatment with SKF96365 at 10 μmol/L for 48 hours significantly increased the proportion of the cells at G2/M and S phases (Figure 3D), which indicated that SKF96365 induced cell-cycle arrest. Taking together, the inhibitory effect on NPC cell growth should also be attributed to the apoptosis enhancing and cell-cycle arresting pharmacological properties of SKF96365.

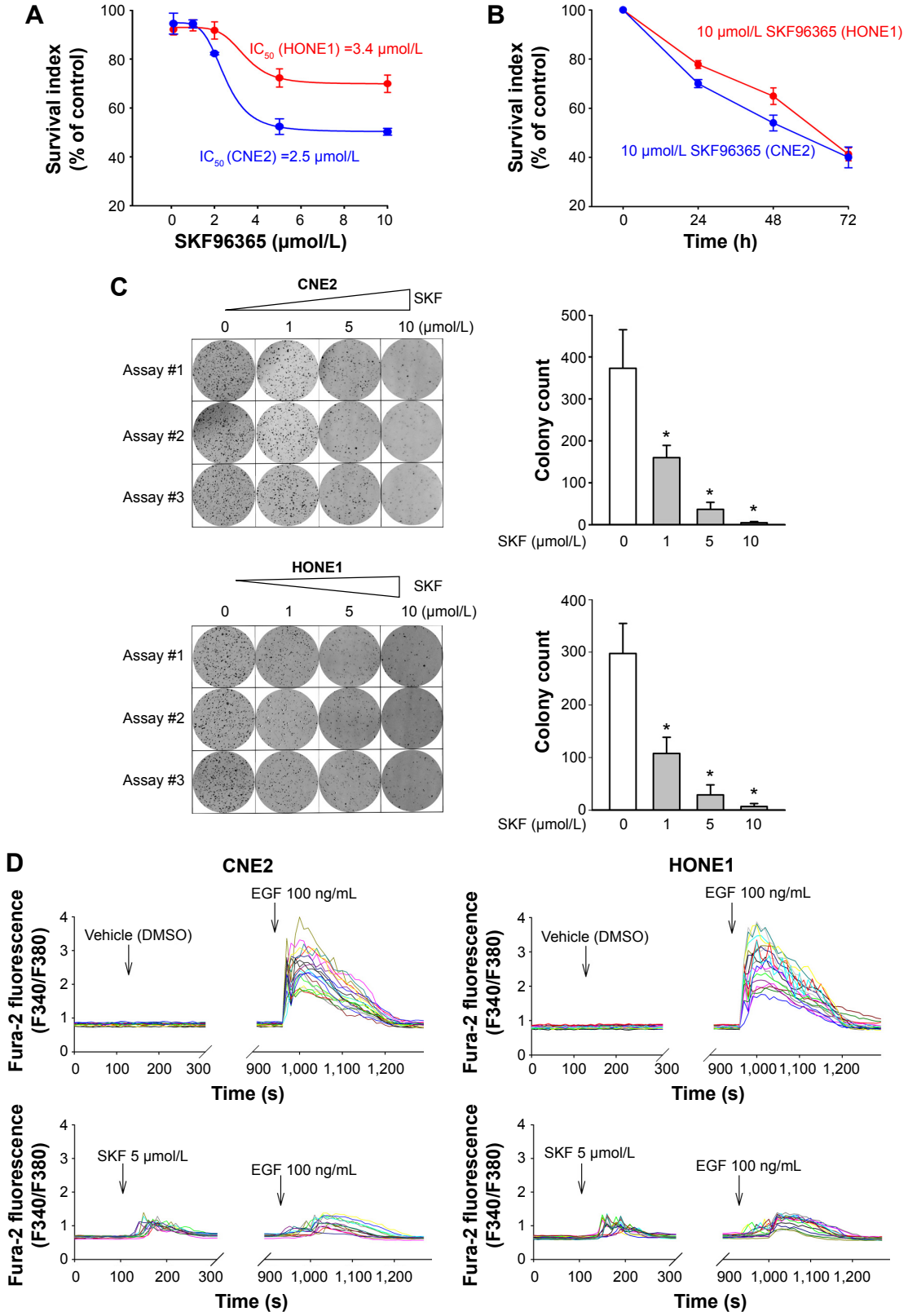

Figure 2 SKF96365 promotes cell mortality and inhibits colony formation while disturbing EGF-evoked Ca^{2+} signaling.

Notes: (**A**) The cells were treated with SKF96365 at the increasing concentrations for 48 h. Effect of SKF96365 at the indicated doses on NPC cell survival is shown as the percent of the untreated cells. (**B**) The cells were treated with SKF96365 for various durations as indicated. (**C**) Effect of SKF96365 at the indicated doses on colony formation. The number of the colonies is shown in each right panel. (**D**) Effect of the preincubation with SKF96365 on EGF-evoked Ca^{2+} responses. The cells were preincubated with SKF96365 at 5 μmol/L or vehicle control (DMSO) for 10 minutes before the application of EGF. Each reaction trace represents the Ca^{2+} responses in each single cell. The traces were individualized by indicating with multiple colors. Data are represented as mean ± SD (*$P<0.05$, Student's *t*-test).

Abbreviations: SKF, SKF96365; EGF, epidermal growth factor; NPC, nasopharyngeal carcinoma; DMSO, dimethyl sulfoxide; IC_{50}, half maximal inhibitory concentration; h, hour(s); s, seconds; SD, standard deviation.

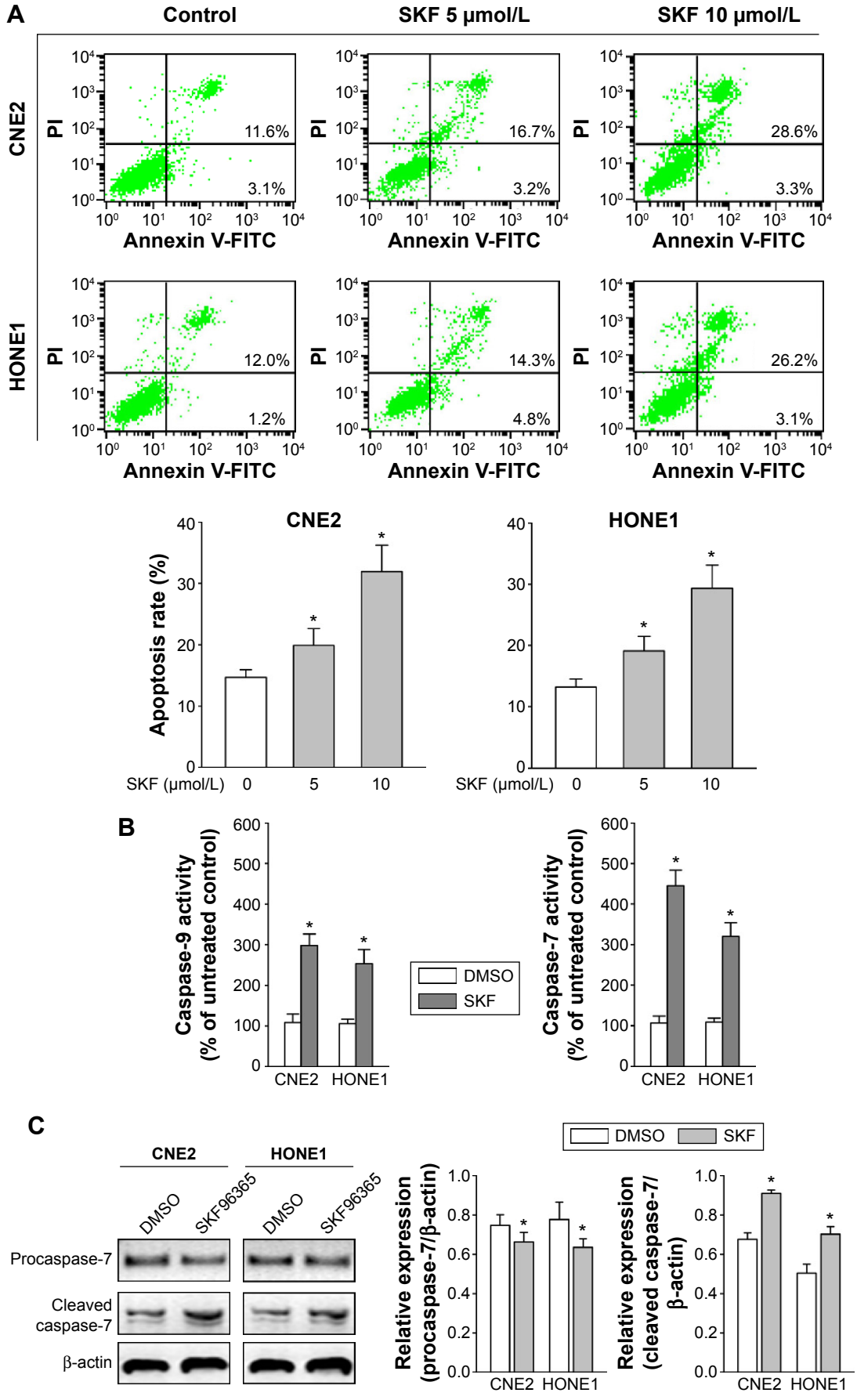

Figure 3 (*Continued*)

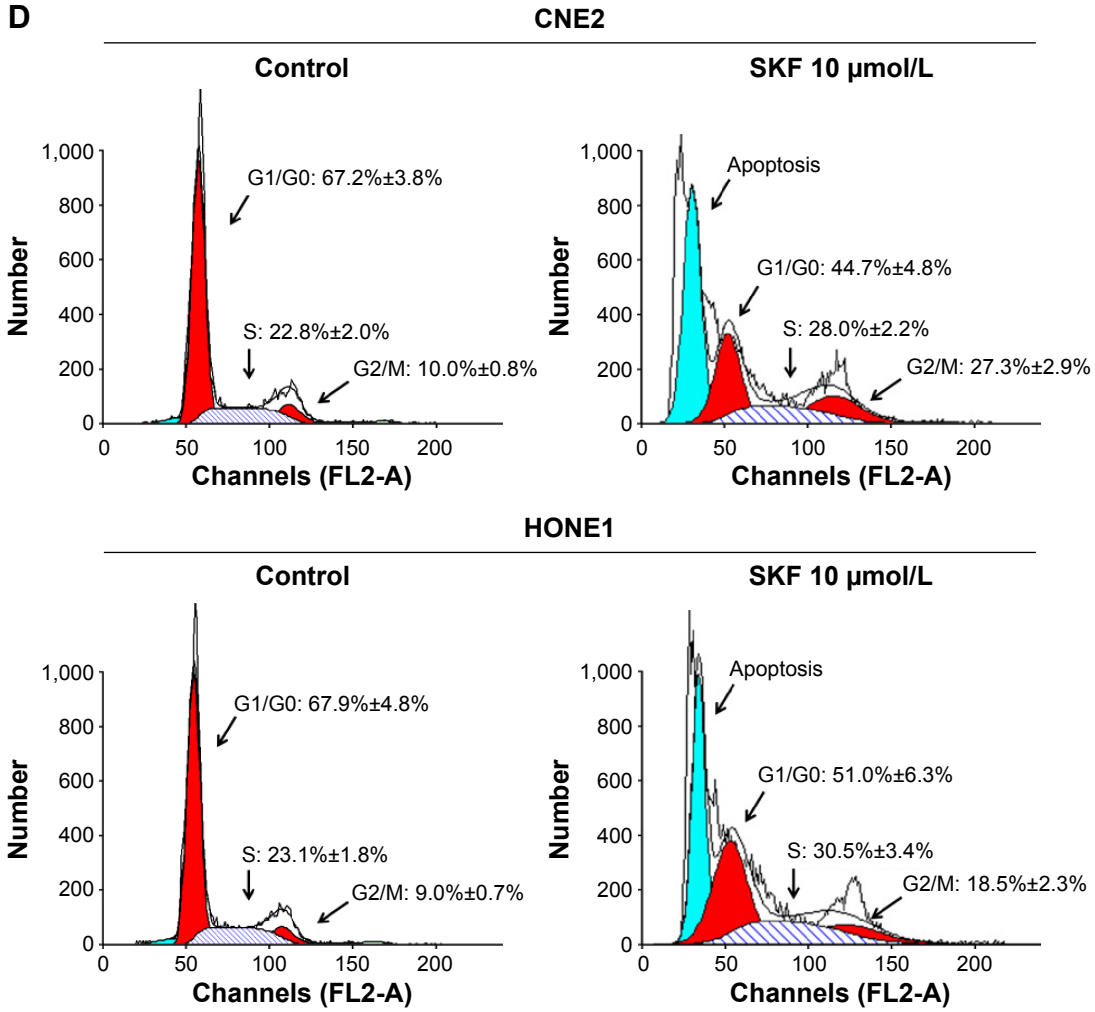

Figure 3 SKF96365 induces apoptosis and cell-cycle arresting.
Notes: (**A**) The representative results of cell apoptosis determined by flow cytometry are shown. The cell apoptosis status in each experimental group is summarized as the percentage of apoptotic cells in the right panels. (**B**) The activities of caspase-9 and caspase-7 were estimated using ELISA. (**C**) Pro- and cleaved caspase-7 expressions were detected by Western blotting. The relative expressions of pro- and cleaved caspase-7 quantified by densitometric analysis are shown in the right panel. (**D**) Cell-cycle stage was examined using flow cytometry. The representative results are shown and the summaries of cell-cycle assays are indicated as the proportions of the cells at G0/G1, G2/M, or S phases. Data are expressed as the mean ± SD of three independent experiments or representative of three independent observations. (*$P<0.05$, Student's *t*-test).
Abbreviations: ELISA, enzyme-linked immunosorbent assay; PI, propidium iodide; DMSO, dimethyl sulfoxide; SKF, SKF96365; SD, standard deviation.

SKF96365 suppresses xenograft growth in mice

The results shown earlier strongly suggested that SKF96365 could exhibit antitumor activity in vivo. We employed a xenograft-bearing mice model to elucidate the antitumor effect of SKF96365. The transplanted tumor burden was estimated by measuring the xenograft volume in mice. The tumor burden in the SKF96365-treated group was significantly reduced as compared with the vehicle control group (Figure 4A). We also recorded the body weight changes of the mice during our observation to elucidate the potential nonspecific toxicity or side effects induced by SKF96365. It was found that injection of SKF96365 did not significantly reduce the mice body weight compared with vehicle control group. Furthermore, immunohistochemical analysis revealed that the cytoplasmic cleaved caspase-7 was highly expressed in the SKF96365-treated xenografts, but almost undetectable in the vehicle-treated xenografts (Figure 4B). The results indicated that SKF96365 could exert antitumor activity in vivo while activating the caspase-7-related apoptotic pathway.

Discussion

EGFR was overexpressed and functionalized by Epstein–Barr virus-encoded latent membrane proteins in NPC cells, and therefore external EGF acts as a crucial extracellular signal molecule that triggers intracellular oncogenic signaling, and thereby facilitating the progression of this human malignancy.[17–20] In our earlier studies, we showed that SOCE

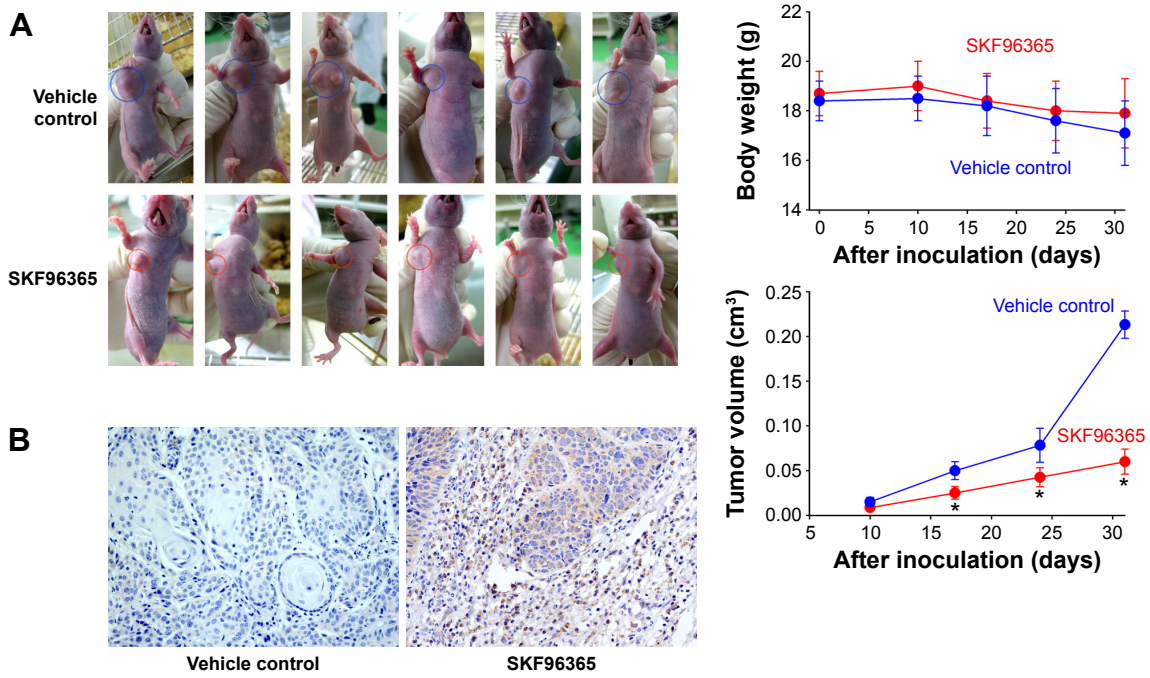

Figure 4 SKF96365 inhibits xenograft growth in mice.
Notes: (**A**) The transplanted tumors in PBS and SKF96365-treated group were captured on day-30 postinoculation. The tumor volumes were measured every seventh day after the palpable xenografts could be observed. The changes of body weight during the experimental observation are shown. Data are represented as mean ± SD (*$P<0.05$, Student's *t*-test). (**B**) The representative immunohistochemical analysis of cleaved caspase-7 in the paraffin-embedded xenograft sections isolated from PBS or SKF96365-treated mice (400× magnification).
Abbreviations: PBS, phosphate-buffered saline; SD, standard deviation.

was a key Ca^{2+} signaling that regulates NPC cell migration,[11] and the amplification of EGF-evoked Ca^{2+} signaling was responsible for the highly metastatic potential in NPC cells.[14] SOCE-mediated Ca^{2+} signaling also actively participates in the multiple steps of other human cancer development.[5–8] Therefore, SOCE is considered to be a candidate target for antitumor therapy.[4]

Utilization of pharmacological inhibitors appears to be an effective intervention to block SOCE.[4] Our previous studies showed that a blocker of SOCE, 2-APB, which suppressed the EGF-stimulated cell migration and VEGF-mediated angiogenesis, only exhibited inhibitory effect on extracellular Ca^{2+} influx.[11,14] As reported by Jan et al, SKF96365 stimulated a transient cytosolic Ca^{2+} response in Madin Darby canine kidney cells only at a high dose range (25–100 µmol/L), while at a lower dose (10 µmol/L) was noneffective.[21] Moreover, SKF96365 not only induced intracellular Ca^{2+} release but also Ca^{2+} influx in Madin Darby canine kidney cells.[21] SKF96365 is a modified econazole, and econazole was also found to induce both ER-released Ca^{2+} and Ca^{2+} influx at a dose range of 5–50 µmol/L.[22] Inconsistently, SKF96365 only induced ER-released Ca^{2+} at 10 µmol/L but could not stimulate Ca^{2+} influx in NPC cells (Figure 1C and D). It may be ascribed to the variable pharmacological characters of SKF96365 in different cell types. In fact, the effects of SKF96365 even differed in the two NPC cell lines in our study. SKF96365 at 5 µmol/L obviously inhibited or even almost blocked the Ca^{2+} influx in HONE1 cells, but SKF96365 at the same dose only mildly affected the Ca^{2+} influx in CNE2 cells (Figure 1A). It might be ascribed to the diverse pharmacological sensibility to SKF96365 in different cell lines. These results suggest that the effects of SKF96365 on Ca^{2+} signaling are complex and variable according to the cell specificity. However, the mechanism by which SKF96365 induces ER-released Ca^{2+} and how to disturb or desynchronized EGF-evoked Ca^{2+} signaling still need to be further established.

In view of that SKF96365 showed dual influences on both ER-released Ca^{2+} and the following Ca^{2+} influx (Figure 1A), we hypothesized that SKF96365 might exert more complex effects on other malignant biological behaviors in NPC cells, such as the deregulation of cell proliferation and resistance to programmed cell death. Indeed, in this study, SKF96365 was found to promote NPC cell mortality. We also showed that SKF96365 apparently blunted the EGF-evoked Ca^{2+} signaling (Figure 2D), the distraction of EGF-signaling transduction presumably contributed to the enhancement of NPC cell mortality (Figure 2A). Furthermore, cytosolic Ca^{2+} is a ubiquitous intracellular second messenger that controls various aspects

of cell-life activities.[1,12,13] We also revealed that SKF96365 inhibited colony formation, induced apoptosis, and cell-cycle arrest at G2/M and S phases. These antitumor properties were not observed in the *Orai1*-knockdown NPC cells, in which Ca^{2+} influx was effectively blocked by the silencing of the key membrane Ca^{2+} pore protein.[14] Hence, the antitumor effects of SKF96365 presented in this study should be attributable to its interference in the intracellular mobilization of Ca^{2+} from ER, which initializes the external stimuli-evoked intracellular signaling transduction.[2,3] Our results showed that SKF96365 only induced slight Ca^{2+} response as compared with that induced by TG, which might be insufficient to activate SOCE (Figure 1C). Therefore, our findings suggest that the antitumor activity of SKF96365 was independent of SOCE. Indeed, although both econazole (such as SKF96365) and sarco/ER Ca^{2+}-ATPase (SERCA) inhibitor (such as TG) can induce ER-released Ca^{2+}, TG toxicity results from mitochondrial Ca^{2+} overload and ER stress highly associated with Ca^{2+} stores depletion, whereas SKF96365 induces cell death through sustained protein synthesis inhibition.[23]

In the present study, we explored the pathway through which SKF96365 promotes apoptosis in NPC cells. Of various caspases, we found that the activities of both caspase-9 and caspase-7 were enhanced in SKF96365-treated cells (Figure 3B). Caspase-7 plays a crucial role in cell apoptosis as an executioner protein. Caspase-7 exists as an inactive proenzyme (procaspase-7) that is able to be activated by upstream caspases, including caspase-9. Thus, our findings suggested that the active caspase-7 awaked by caspase-9 was implicated in the SKF96365-triggered apoptosis process. We confirmed that SKF96365 significantly increased cleaved caspase-7 and decreased procaspase-7 expression (Figure 3C), which indicated that the conversion of inactive procaspase-7 to active cleaved caspase-7 actively participated in the SKF96365-induced apoptosis. However, the pathway through which SKF96365 modulates caspase-9 remains poorly understood and still remains to be clarified.

To test the in vivo antitumor activity of SKF96365 in xenograft-bearing mice, we evaluated the tumor burden in SKF96365-treated mice in comparison with the vehicle-control mice. Consistent with our in vitro results, SKF96365 reduced the NPC xenograft growth while activating caspase-7-related apoptotic pathway (Figure 4A and B). However, whether SKF96365 inhibits NPC tumor growth through caspase-7-related apoptotic pathway in vivo still remains to be further confirmed by either knockdown strategy or using pharmacological inhibitor. On the other hand, the reduction of xenograft growth might also result from a global proapoptotic nature or nonspecific toxicity of SKF96365. In this study, we found that SKF96365 had no signs of overt toxicity or significant effects on body weight changes of mice, suggesting the dosage regimen of SKF96365 used in the present study was generally well tolerated, which was consistent with a previous study.[8] Since SKF96365 is considered to be a broad spectrum inhibitor, the antitumor effects of other highly selective inhibitors (such as Synta66, GSK-7975A, and BTP2) of SOCE should be further evaluated in NPC cells.

Conclusion

The findings shown in this study indicated that SKF96365 exhibited various antitumor activities, such as the promotion of cell mortality, inhibition of colony formation, inductions of apoptosis, and cell-cycle arrest in NPC cells. These antitumor effects could be ascribed to the disturbance of cytosolic Ca^{2+} signaling, as a result of the dual impacts of SKF96365 on ER-released Ca^{2+} and the following Ca^{2+} influx.

Acknowledgments

This study was supported by grants from the National Natural Scientific Foundation of China (numbers 81560438, 81272983, and 81260404), Guangxi Natural Science Foundation (numbers 2015GXNSFCA139014, 2013GXNSFGA019002), Program for New Century Excellent Talents in University (number NCET-12-0654), Key Project of Health Department of Guangxi Province (number 200919), and Youth Science Foundation of Guangxi Medical University (number GXMUYSF201403).

Disclosure

The authors report no conflicts of interest in this work.

References

1. Clapham DE. Calcium signaling. *Cell*. 2007;131(6):1047–1058.
2. Parekh AB, Penner R. Store depletion and calcium influx. *Physiol Rev*. 1997;77(4):901–930.
3. Parekh AB, Putney JW Jr. Store-operated calcium channels. *Physiol Rev*. 2005;85(2):757–810.
4. Roberts-Thomson SJ, Peters AA, Grice DM, Monteith GR. ORAI-mediated calcium entry: mechanism and roles, diseases and pharmacology. *Pharmacol Ther*. 2010;127(2):121–130.
5. McAndrew D, Grice DM, Peters AA, et al. ORAI1-mediated calcium influx in lactation and in breast cancer. *Mol Cancer Ther*. 2011;10(3):448–460.
6. Chen YT, Chen YF, Chiu WT, et al. Microtubule-associated histone deacetylase 6 supports the calcium store sensor STIM1 in mediating malignant cell behaviors. *Cancer Res*. 2013;73(14):4500–4509.
7. Chen YF, Chiu WT, Chen YT, et al. Calcium store sensor stromal-interaction molecule 1-dependent signaling plays an important role in cervical cancer growth, migration, and angiogenesis. *Proc Natl Acad Sci U S A*. 2011;108(37):15225–15230.

8. Yang S, Zhang JJ, Huang XY. Orai1 and STIM1 are critical for breast tumor cell migration and metastasis. *Cancer Cell*. 2009;15(2):124–134.
9. Vokes EE, Liebowitz DN, Weichselbaum RR. Nasopharyngeal carcinoma. *Lancet*. 1997;350(9084):1087–1091.
10. Tao Q, Chan AT. Nasopharyngeal carcinoma: molecular pathogenesis and therapeutic developments. *Expert Rev Mol Med*. 2007;9(12):1–24.
11. Zhang J, Wei J, Kanada M, et al. Inhibition of store-operated Ca2+ entry suppresses EGF-induced migration and eliminates extravasation from vasculature in nasopharyngeal carcinoma cell. *Cancer Lett*. 2013;336(2):390–397.
12. Berridge MJ, Bootman MD, Roderick HL. Calcium signalling: dynamics, homeostasis and remodelling. *Nat Rev Mol Cell Biol*. 2003;4(7):517–529.
13. Roderick HL, Cook SJ. Ca2+ signalling checkpoints in cancer: remodelling Ca2+ for cancer cell proliferation and survival. *Nat Rev Cancer*. 2008;8(5):361–375.
14. Wei J, Zhang J, Si Y, et al. Blockage of LMP1-modulated store-operated Ca(2+) entry reduces metastatic potential in nasopharyngeal carcinoma cell. *Cancer Lett*. 2015;360(2):234–244.
15. Wei J, Takeuchi K, Watanabe H. Linoleic acid attenuates endothelium-derived relaxing factor production by suppressing cAMP-hydrolyzing phosphodiesterase activity. *Circ J*. 2013;77(11):2823–2830.
16. Lin Y, Liu Z, Li Y, et al. Short-term hyperthermia promotes the sensitivity of MCF-7 human breast cancer cells to paclitaxel. *Biol Pharm Bull*. 2013;36(3):376–383.
17. Miller WE, Earp HS, Raab-Traub N. The Epstein-Barr virus latent membrane protein 1 induces expression of the epidermal growth factor receptor. *J Virol*. 1995;69(7):4390–4398.
18. Thornburg NJ, Raab-Traub N. Induction of epidermal growth factor receptor expression by Epstein-Barr virus latent membrane protein 1 C-terminal-activating region 1 is mediated by NF-kappaB p50 homodimer/Bcl-3 complexes. *J Virol*. 2007;81(23):12954–12961.
19. Kung CP, Raab-Traub N. Epstein-Barr virus latent membrane protein 1 induces expression of the epidermal growth factor receptor through effects on Bcl-3 and STAT3. *J Virol*. 2008;82(11):5486–5493.
20. Kung CP, Meckes DG Jr, Raab-Traub N. Epstein-Barr virus LMP1 activates EGFR, STAT3, and ERK through effects on PKCdelta. *J Virol*. 2011;85(9):4399–4408.
21. Jan CR, Ho CM, Wu SN, Tseng CJ. Multiple effects of 1-[beta-[3-(4-methoxyphenyl)propoxy]-4-methoxyphenethyl]-1H-imidazole hydrochloride (SKF 96365) on Ca2+ signaling in MDCK cells: depletion of thapsigargin-sensitive Ca2+ store followed by capacitative Ca2+ entry, activation of a direct Ca2+ entry, and inhibition of thapsigargin-induced capacitative Ca2+ entry. *Naunyn Schmiedebergs Arch Pharmacol*. 1999;359(2):92–101.
22. Jan CR, Ho CM, Wu SN, Tseng CJ. Multiple effects of econazole on calcium signaling: depletion of thapsigargin-sensitive calcium store, activation of extracellular calcium influx, and inhibition of capacitative calcium entry. *Biochim Biophys Acta*. 1999;1448(3):533–542.
23. Soboloff J, Berger SA. Sustained ER Ca2+ depletion suppresses protein synthesis and induces activation-enhanced cell death in mast cells. *J Biol Chem*. 2002;277(16):13812–13820.